HHS Public Access

Author manuscript

Nat Immunol. Author manuscript; available in PMC 2018 January 01.

Published in final edited form as:

Nat Immunol. 2017 January ; 18(1): 45–53. doi:10.1038/ni.3630.

TET proteins regulate the lineage specification and TCR-mediated expansion of *i*NKT cells

Ageliki Tsagaratou[1], **Edahí González-Avalos**[1,8], **Sini Rautio**[2,8], **James P Scott-Browne**[1,3], **Susan Togher**[1], **William A Pastor**[1,7], **Ellen V Rothenberg**[4], **Lukas Chavez**[5], **Harri Lähdesmäki**[2], and **Anjana Rao**[1,3,6]

[1]Department of Signaling and Gene Expression, La Jolla Institute for Allergy and Immunology, La Jolla, California, USA [2]Department of Computer Science, Aalto University School of Science, Aalto, Finland [3]Sanford Consortium for Regenerative Medicine, La Jolla, California, USA [4]Division of Biology and Biological Engineering, California Institute of Technology, Pasadena, California, USA [5]Division of Pediatric Neurooncology, German Cancer Research Center (DKFZ), Heidelberg, Germany [6]Department of Pharmacology and Moores Cancer Center, University of California at San Diego, La Jolla, California, USA

Abstract

TET proteins oxidize 5-methylcytosine in DNA to 5-hydroxymethylcytosine and other oxidation products. We found that simultaneous deletion of *Tet2* and *Tet3* in mouse $CD4^+CD8^+$ double-positive thymocytes resulted in dysregulated development and proliferation of invariant natural killer T cells (*i*NKT cells). *Tet2*-*Tet3* double-knockout (DKO) *i*NKT cells displayed pronounced skewing toward the NKT17 lineage, with increased DNA methylation and impaired expression of genes encoding the key lineage-specifying factors T-bet and ThPOK. Transfer of purified *Tet2*-*Tet3* DKO *i*NKT cells into immunocompetent recipient mice resulted in an uncontrolled expansion that was dependent on the nonclassical major histocompatibility complex (MHC) protein CD1d, which presents lipid antigens to *i*NKT cells. Our data indicate that TET proteins regulate *i*NKT cell fate by ensuring their proper development and maturation and by suppressing aberrant proliferation mediated by the T cell antigen receptor (TCR).

Correspondence should be addressed to A.R. (arao@lji.org).

[7]Present address: Department of Molecular, Cell and Developmental Biology, University of California at Los Angeles, Los Angeles, California, USA.

[8]These authors contributed equally to this work.

Note: Any Supplementary Information and Source Data files are available in the online version of the paper.

AUTHOR CONTRIBUTIONS

A.R. and A.T. designed the study; A.T. performed all of the experiments, and A.R. and A.T. wrote the manuscript. E.G.-A. analyzed WGBS and ATAC-seq data sets under the supervision of L.C. and J.P.S.-B., respectively. S.R. analyzed RNA-seq and CMS-IP data sets under the supervision of H.L. S.T. helped with *in vivo* adoptive transfer experiments. W.A.P. generated the $Tet3^{fl/fl}$ mice. E.V.R. provided critical input and suggestions during the course of this study and helped write the manuscript.

COMPETING FINANCIAL INTERESTS

The authors declare no competing financial interests.

T cell development is tightly regulated by transcription factors that dictate lineage commitment[1,2]. The DNA-binding transcription factors Foxp3, Runx3, ThPOK and PLZF orchestrate the cell-specific transcriptional programs of regulatory T cells (T_{reg} cells), $CD8^+$ single-positive (CD8SP) T cells, $CD4^+$ single-positive (CD4SP) T cells and *i*NKT cells, respectively[2,3]. Transcription factors also control the further differentiation of peripheral naive $CD4^+$ T cells into the T_H1 subset of helper T cells that expresses the transcription factor T-bet, T_H2 cells that express the transcription factor GATA-3 and T_H17 cells that express the transcription factor RORγt[4].

Whereas conventional T cells are selected by peptide antigens presented on MHC class I and II proteins, *i*NKT cells are positively selected in the thymus through recognition of lipid antigens presented by the nonclassical MHC-class-I-like protein CD1d[3], and their differentiation is induced by strong TCR signaling through agonist selection[5]. *i*NKT cells are defined by their ability to bind CD1d–α-galactosyl-ceramide tetramers (called simply 'tetramers' here) and are subdivided into four stages on the basis of their expression of surface markers: stage 0 *i*NKT precursors have high expression of the B cell–differentiation marker CD24; stage 1 cells have undergone positive selection and massive proliferation and downregulate CD24 expression; stage 2 cells continue proliferating and upregulate expression of the activation and memory marker CD44, but do not express the activating NK cell receptor NK1.1; and stage 3 cells are $CD44^+NK1.1^+$ (ref. 3).

An alternative transcription-factor-centered classification categorizes *i*NKT cells that express T-bet and secrete interferon-γ (IFN-γ) as NKT1 cells; *i*NKT cells that express GATA-3 and secrete mostly interleukin 4 (IL-4) as NKT2 cells; and *i*NKT cells that express RORγt and produce IL-17 as NKT17 cells (ref. 6). Phenotypically, NKT1 cells are $PLZF^{lo}NK1.1^+$ and have been described as 'stage 3′ cells[3], whereas NKT2 and NKT17 cells are characterized by the lack of NK1.1 expression[3] and therefore fall into stage 2 of *i*NKT cell development. These three lineages are distinct, as they do not interconvert when they are injected intrathymically[6].

Gene expression is subject to epigenetic regulation by histone and DNA modifications, nucleosome positioning, chromatin remodeling, and long-range chromatin interactions, which collectively affect the binding of transcription factors to their consensus sequences in DNA[7,8]. Among the most recently discovered epigenetic modifiers are the TET-family dioxygenases TET1, TET2 and TET3, which catalyze the oxidation of 5-methylcytosine (5mC) in DNA to 5-hydroxymethylcytosine (5hmC) and other oxidation products[9–11]. These modified bases are intermediates in DNA demethylation as well as epigenetic marks that may recruit specific readers[12].

Dynamic changes in the distribution of 5hmC during thymic T cell lineage specification have been reported[13]. Here we found that deletion of both *Tet2* and *Tet3* in mice resulted in a lethal lymphoproliferative disease characterized by massive antigen-dependent expansion of *i*NKT cells. The disease was recapitulated by the transfer of small numbers of highly purified *Tet2-Tet3* DKO *i*NKT cells into fully immunocompetent wild-type recipient mice, but could not be recapitulated by the transfer of such cells into CD1d-deficient recipient mice, which indicated that the *i*NKT cell expansion was driven by antigen recognition and

TCR signaling. In parallel, we observed a pronounced skewing toward the NKT17 lineage, which correlated with increased DNA methylation and decreased expression of lineage-specifying transcription factors such as T-bet and ThPOK. Overall, our data indicate that TET2 and TET3 are important regulators of *i*NKT cell development and lineage specification, as well as tumor suppressors that restrict TCR-driven expansion.

RESULTS

*i*NKT cell expansion in *Tet2-Tet3* DKO mice

TET2 and TET3 are the main TET proteins expressed in mouse T cells[14]. *Tet2*$^{-/-}$ mice[15] are healthy and show no defects in T cell development, but *Tet3*$^{-/-}$ mice display perinatal death[16]. To evaluate the effect of deletion of both *Tet2* and *Tet3*, we crossed *Tet3*$^{fl/fl}$*Cd4-Cre* (*Tet3* KO) mice (in which *lox*P-flanked Tet3 alleles (*Tet3*$^{fl/fl}$) are deleted by Cre recombinase expressed from the T cell–specific *Cd4* promoter (*Cd4-Cre*)) with *Tet2*$^{-/-}$ mice. Deletion of the *Tet2* and *Tet3* exons in T cells was confirmed by quantitative PCR; there was no compensatory upregulation of *Tet1* mRNA (Supplementary Fig. 1a). Global 5hmC content was considerably lower, but was not eliminated, in sorted double-positive (DP), CD4SP and CD8SP thymocytes of *Tet2*$^{-/-}$ *Tet3*$^{fl/fl}$*Cd4-Cre* (*Tet2-Tet3* DKO mice) than in the corresponding subsets of wild-type mice (Supplementary Fig. 1b). Although most of our experiments were performed with *Tet2*$^{-/-}$ *Tet3*$^{fl/fl}$*Cd4-Cre* mice, we observed identical phenotypes in *Tet2*$^{fl/fl}$ *Tet3*$^{fl/fl}$*Cd4-Cre* mice (data not shown).

Beginning at 5 weeks of age, all *Tet2-Tet3* DKO mice lost weight and exhibited a bloated and hunched appearance, whereas *Tet2*$^{-/-}$ and *Tet3* KO mice remained healthy up to 14 months (data not shown). Within a few weeks of birth, *Tet2-Tet3* DKO mice developed enlarged spleens and lymph nodes (data not shown), with disrupted architecture and loss of germinal centers (Supplementary Fig. 1c). The lungs and livers of *Tet2-Tet3* DKO mice showed pronounced lymphocyte infiltration (Supplementary Fig. 1c). By 5–7 weeks, spleen cellularity was substantially increased (Fig. 1a), and all of the mice succumbed by 8 weeks of age (Fig. 1b). Disease development was associated with a massive expansion of *i*NKT cells in spleen and lymph nodes, even in young mice that maintained a normal reservoir of T_{reg} cells (Fig. 1c,d); single deletion of *Tet2* or *Tet3* had a small, but significant, effect (Fig. 1e,f and Supplementary Fig. 1d,e). Moreover, compared with their wild-type counterparts, 3–4-week-old *Tet2-Tet3* DKO mice showed decreased thymic cellularity and decreased percentages and numbers of DP thymocytes, suggestive of intrathymic stress, as well as a relative increase in the number and frequency of CD4SP and CD8SP cells in the thymus (Supplementary Fig. 2a–d). In contrast, peripheral lymphoid organs (spleen and lymph nodes) showed greatly increased cellularity despite decreased frequencies of peripheral $CD4^+$ and $CD8^+$ T cells (Supplementary Fig. 2e–h). Overall, simultaneous loss of Tet2 and Tet3 resulted in *i*NKT cell expansion and lethal disease.

Regulation of *i*NKT-cell-lineage specification by TET2 and TET3

Notably, the selective expansion of *Tet2-Tet3* DKO *i*NKT cells was already apparent in the thymus of very young (20-day-old) *Tet2-Tet3* DKO mice (Fig. 2a–c). The percentages and absolute numbers of thymic *i*NKT cells were much greater in *Tet2-Tet3* DKO mice than in

wild-type, *Tet2*$^{-/-}$ or *Tet3* KO mice (Supplementary Fig. 3a,b). Compared with *i*NKT cells of the other genotypes, *Tet2-Tet3* DKO *i*NKT cells showed increased expression of RORγt in the thymus and periphery and loss of CD4 expression, which suggested skewing toward an NKT17-like phenotype[6]; decreased expression of *Tbet* in the thymus, which reflected a decrease in the number of NKT1-lineage cells; and increased expression of PLZF, consistent with a reduction in the number of cells of the NKT1 cell (PLZF^{lo}) lineage (Fig. 2d,e and Supplementary Fig. 3). In wild-type mice, more than 60% of *i*NKT cells were NKT1 cells, whereas the predominant NKT cell subtype in *Tet2-Tet3* DKO mice was NKT17 (Fig. 2f). However, because of the prominent *i*NKT cell expansion in the thymus, all effector *i*NKT cell subtypes were overrepresented in thymocytes of *Tet2-Tet3* DKO relative to their abundance in wild-type mice (Fig. 2g).

Consistent with their skewing toward the NKT17 cell lineage, *Tet2-Tet3* DKO *i*NKT cells potently produced IL-17 when stimulated with phorbol 12-myristate 13-acetate (PMA) and ionomycin (Supplementary Fig. 4a–c). The frequency of IFN-γ-producing *i*NKT cells was diminished relative to wild type, but, as a result of the *i*NKT cell expansion, the percentage of IFN-γ-producing *i*NKT cells among total thymocytes was increased (Supplementary Fig. 4d–f). This was also observed for IL-4 (Supplementary Fig. 4g–i). Relative to wild type, the increased numbers of PLZF^{hi}, IL-4 producing *i*NKT cells in *Tet2-Tet3* DKO mice were associated with the expected increase in numbers of innate-like memory CD8SP cells[17] (Supplementary Fig. 4j,k), which showed high expression of genes associated with an activated, memory-like phenotype (data not shown). *Tet2-Tet3* DKO CD8^{+} cells were underrepresented in the periphery (Supplementary Fig. 2e–h), presumably as a result of defects in migration and/or survival. We focused on the aberrant *i*NKT cells in *Tet2-Tet3* DKO mice.

Tetramer^{hi}NK1.1^{-} cells, which normally include CD4^{+}CD27^{+} NKT2 cells[6], NKT17 cells that do not express CD4 (ref. 6) and NKT1 precursor cells identified by T-bet expression[18], were greater in terms of both percentage and absolute numbers in *Tet2-Tet3* DKO mice than in wild-type mice (Fig. 2h–j). CD4 expression was almost undetectable in *Tet2-Tet3* DKO *i*NKT cells, in contrast to its detectable expression in wild-type *i*NKT cells (Fig. 2h and Supplementary Fig. 3c). There was also a much larger PLZF^{+}RORγt^{+} population in the NK1.1^{-} *Tet2-Tet3* DKO subset than in its wild-type counterpart (Supplementary Fig. 5a,b), with a concomitant decrease in the PLZF^{+}T-bet^{+} subset that is thought to contain precursors of NKT1-cell-lineage cells (Supplementary Fig. 5c,d). Compared with their wild-type counterparts, a small population of *Tet2-Tet3* DKO tetramer^{+}NK1.1^{+}CCR6^{-}CD27^{+} NKT1 cells exhibited higher expression of PLZF than that of their their wild-type counterparts and aberrant expression of RORγt, and a small fraction of this PLZF^{hi} population did not express T-bet (Supplementary Fig. 5e). The NK1.1^{+} *Tet2-Tet3* DKO *i*NKT cells were not only less frequent among the thymic *i*NKT cells than their wild-type counterparts, but they were also functionally compromised, as they produced less IFN-γ than did wild-type cells (Supplementary Fig. 5f,g). We concluded that Tet2 and Tet3 regulated the generation and maturation of these *i*NKT cell lineages.

NKT17 lineage skewing in *Tet2-Tet3* DKO *i*NKT cells

Transcriptional profiling of total thymic *i*NKT cells confirmed skewing toward the NKT17 cell lineage, with *i*NKT cells from young (3- to 4-week-old) *Tet2-Tet3* DKO mice showing higher expression of *Il17f*, *Rorc* (which encodes RORγt) and *Eomes* and lower expression of *Ifng*, *Il4*, *Tbx21* (which encodes T-bet) and *Zbtb7b* (which encodes ThPOK) than wild-type *i*NKT cells (Fig. 3a,b). We also observed higher expression of *Lef1*, which can promote malignant transformation[19]; *Rag1*, whose expression in NK cells correlates with an enhanced fitness, proliferative and survival capacity[20]; and the oncogenes *Lmo4* (ref. 21) and *Myb*[22] (Fig. 3a). These genes normally have high expression in DP thymocytes and are progressively downregulated[1], which indicates that Tet2-Tet3 deficiency results in developmental immaturity.

We also compared subtypes of wild-type and *Tet2-Tet3* DKO *i*NKT cells (Fig. 3c). Genes that were downregulated in *Tet2-Tet3* DKO stage 0 *i*NKT precursors relative to their expression in wild-type cells included those encoding CD4, Bcl11b (which restricts the NKT17 lineage[23]) and Satb1 (which forms complexes with PLZF in the presence of the Cullin E3 ligase[24]); genes that were upregulated included *Zbtb16* (which encodes PLZF) and *Lmo4* (Fig. 3c). In the heterogeneous NK1.1^{-} *i*NKT cell population, genes that were upregulated in *Tet2-Tet3* DKO cells relative to their expression in wild-type cells included *Rorc*, *Zbtb16* and *Myc* (whose product controls *i*NKT cell proliferation[25]), and genes that were downregulated included *Cd4*, *Satb1*, *Tbx21* and *Zbtb7b* (Fig. 3c). Combined loss of *Tet2* and *Tet3* affected the number, maturation and identity of the generated NKT1 cells; among the upregulated genes that we identified, *Rorc* and *Lef1* (which is usually upregulated at an earlier stage (stage 0) of *i*NKT cell development)[18] were expressed in stage 1 and 2 *i*NKT cells but are normally absent in stage 3 *i*NKT cells[26]. Thus, TET2 and TET3 markedly affect the gene-expression profiles of all *i*NKT cell subsets.

Enhanced proliferation of *Tet2-Tet3* DKO *i*NKT cells

The upregulation of *Myc*, *Rag1*, *Lmo4*, *Myb* and other genes associated with the *i*NKT precursor state and high proliferative capacity prompted us to assess the proliferation of *Tet2-Tet3* DKO *i*NKT cells *in vivo*. We injected mice with BrdU, a thymidine analog that is incorporated into DNA during replication, and analyzed *i*NKT cells 16 h later. Indeed, *Tet2-Tet3* DKO *i*NKT cells showed significantly higher BrdU incorporation than did wild-type thymic *i*NKT cells (Fig. 3d,e).

Given that T_{reg} cell function is compromised in *Tet2-Tet3* DKO mice[27], we sought to determine whether uncontrolled *i*NKT cell expansion would occur in the presence of intact T_{reg} cells and, if so, whether antigen recognition would be involved. We transferred total *Tet2-Tet3* DKO splenocytes (data not shown) or purified *Tet2-Tet3* DKO *i*NKT cells (5×10^5) into fully immunocompetent (non-irradiated) CD45.1^{+} recipient mice, either wild-type or lacking CD1d. All wild-type recipients developed enlarged spleen and lymph nodes and succumbed to disease by 90 d, whereas all CD1d-deficient (CD1d KO) recipients remained healthy (Fig. 4a). Spleen and lymph node cellularity increased significantly in the recipient mice, to an average of ~5×10^8 cells after transfer (Fig. 4b); of these, typically >80% were

*i*NKT cells (Fig. 4c). We also observed a slight expansion in CD1d KO recipients (Fig. 4b,c).

Compared with the expression of these genes in wild-type *i*NKT cells (Fig. 4d), transferred *Tet2-Tet3* DKO *i*NKT cells maintained their expression of *Rorc* and *Myb*, upregulated their expression of genes encoding transcriptional regulators and oncogenic factors indicative of earlier stages of T cell development (*Lmo1* and *Lmo2* (ref. 21), *Tcf7* and *Myc*[28,29]), as well as genes such as *Ret*[30], whose products improve hematopoietic stem cell expansion and transplantation efficiency (Fig. 4d,e). Pathway-enrichment analysis revealed two main categories of differentially expressed genes: those encoding products related to T cell function and those encoding products related to DNA replication, cell cycle and DNA damage repair (Fig. 4f). Together these data indicated that loss of function of TET proteins conferred a cell-intrinsic phenotype of uncontrolled *i*NKT cell proliferation that was driven by antigen recognition and could be observed in recipient mice with normal immunological and T_{reg} cell function.

TET2 and TET3 regulate chromatin accessibility

5hmC mapping by immunoprecipitation of DNA fragments containing cytosine-5-methylenesulfonate, the product of the reaction of 5hmC with sodium bisulfite (CMS-IP)[31,32]. revealed that the greatest amounts of 5hmC in wild-type *i*NKT cells were present in the gene bodies of the genes with the highest expression (Fig. 5a,b), as has been shown for other T cell types[13]. Whole-genome bisulfite sequencing (WGBS) of wild-type *i*NKT cells confirmed the expected inverse correlation between gene expression and DNA modification (5mC+5hmC) at promoters and transcription start sites (TSS)[33] and revealed that loss of 5mC+5hmC extended deeply into the gene bodies of the genes with the greatest transcription (Fig. 5c). Relative to the abundance of 5mC and/or 5hmC at enhancers identified in embryonic stem cells or in cardiac tissue, thymus-specific enhancers[34] showed greater enrichment for 5hmC[13] (472 of 5,605 thymic enhancers intersect with 5hmC; Fig. 5d). Their and their 5mC+5hmC content was greater in *Tet2-Tet3* DKO *i*NKT cells than in wild-type *i*NKT cells (Fig. 5e). Our data indicated that TET proteins were needed continuously to constrain CpG methylation of these enhancers in *i*NKT cells.

Comparing wild-type and young *Tet2-Tet3* DKO *i*NKT cells, we found a much greater average abundance of 5mC+5hmC at the TSS and in gene bodies of *Tet2-Tet3* DKO *i*NKT cells than in those of wild-type cells, whether we considered all genes (data not shown) or only differentially expressed genes (Supplementary Fig. 6a). The increase was specific, as it was not seen in randomly chosen genome fragments of similar size (Supplementary Fig. 6a). Both upregulated genes and downregulated genes in *Tet2-Tet3* DKO *i*NKT cells showed similar increases 5mC+5hmC at promoters and TSSs, as well as gene-body modifications (Supplementary Fig. 6b). Similar findings have been reported for *Tet2-Tet3* DKO hematopoietic stem cells and precursor cells[35]. Overall, although it was clear that TET proteins regulated DNA modification in transcribed regions of the genome (promoters, gene bodies and enhancers), our data suggested a complex relationship between loss of TET protein function, the resulting increase in DNA methylation and changes in gene expression.

Nevertheless, our data suggested involvement of TET proteins in developmental transitions in lymphocytes. Comparing our WGBS data for wild-type *i*NKT cells with data for common lymphoid progenitor (CLP) cells[36], we identified differentially methylated regions (DMRs) whose modification status changed during the differentiation of CLP cells into *i*NKT cells (Fig. 6a). 2,100 regions gained 5mC+5hmC and 1,400 DMRs lost 5mC+5hmC. Focusing on differentiation-related DMRs that lost 5mC+5hmC during the CLP–to–*i*NKT cell transition, we found that *Tet2-Tet3* DKO *i*NKT cells showed increased modification at these DMRs (Fig. 6a), which indicated that loss of 5mC+5hmC during the CLP–to–*i*NKT cell transition required TET2 and TET3. Even in regions that gained modification as CLPs differentiated into *i*NKT cells, DNA modification increased further in *Tet2-Tet3* DKO *i*NKT cells (Fig. 6a), which suggested that cytosine methylation by DNA methyltransferases at these regions was unhindered in the absence of TET2 and TET3. All three TET proteins had higher expression in *i*NKT cells than in CLP cells[37] (Fig. 6b).

We compared the genome-wide distribution of all DMRs with that of 5hmC. Two thirds of all DMRs, whether more highly modified in *Tet2-Tet3* DKO *i*NKT cells or in wild-type *i*NKT cells, were located distal to promoter-TSS regions (that is, more than 5 kb from the TSS; Fig. 6c). Of a total of 10,945 DMRs (Table 1) that were more methylated (5mC +5hmC) in *Tet2-Tet3* DKO *i*NKT cells than in wild-type cells, ~42% overlapped with regions that contained 5hmC in wild-type *i*NKT cells; of these, ~32% were near TSSs (±5 kb), corresponding to a total of 1,270 genes (Table 1). Only 183 (~14%) of these genes showed altered expression (Table 1). These results supported the idea that a subset of 5hmC-bearing promoters in wild-type cells acquire more 5mC+5hmC in the absence of TET function and that a small fraction of the corresponding genes show the expected correlation between increased promoter methylation and decreased expression. A caveat for this is that part, or all, of the modification that we measured might have been a result of 5hmC deposited by TET1.

Finally, we observed a strong correlation between 5hmC distribution and chromatin accessibility, as judged by assay of transposase-accessible chromatin sequencing (ATAC-seq)[38] (Fig. 7). Although similar numbers of genomic regions gained and lost accessibility in *Tet2-Tet3* DKO *i*NKT cells relative to their accessibility in wild-type cells (3,162 and 2,711, respectively), there was a marked overlap (37.5%) between differentially accessible regions (DARs) that lost accessibility in DKO *i*NKT cells and those that had 5hmC in wild-type *i*NKT cells (Fig. 7). In contrast, only a few regions (2.7%) that gained accessibility in *Tet2-Tet3* DKO *i*NKT cells relative to their accessibility in wild-type cells were marked by 5hmC in wild-type *i*NKT cells (Fig. 7a). A considerably smaller fraction of DARs than of DMRs were located close to TSS (Fig. 7b). Most DARs were located far from the TSS, whether they were less accessible in *Tet2-Tet3* DKO *i*NKTs, more accessible in *Tet2-Tet3* DKO iNKTs, or commonly accessible in both wild-type and *Tet2-Tet3* DKO *i*NKTs. Overall, these data suggested a link between the loss of chromatin accessibility in *Tet2-Tet3* DKO *i*NKT cells and the loss of 5hmC.

Regulation of *i*NKT-cell-lineage-specifying factors

Tet2-Tet3 deficiency affected the chromatin accessibility and DNA-modification status of several genes encoding products involved in *i*NKT cell lineage specification and function (Supplementary Figs. 7 and 8). For example, a region near the TSS and first intron of *Zbtb7b* showed both a gain of 5mC+5hmC and a decrease in accessibility in *Tet2-Tet3* DKO relative to such features in wild-type cells, *Tet2-Tet3* DKO *i*NKT cells; note the large undermethylated canyon[39] in the *Zbtb7b* proximal promoter that gains 5mC+5hmC at its edges (Supplementary Fig. 7a). Similarly, a region 5′ of the *Tbx21* promoter that overlaps with a predicted thymic-specific enhancer[34] showed a perceptible gain of 5mC+5hmC and there was a concomitant decrease in *Tbx21* mRNA expression in young *Tet2-Tet3* DKO relative to its expression in wild-type *i*NKT cells (Supplementary Fig. 7b). Moreover, an intragenic region in *Tbx21* that overlaps a different predicted thymus-specific enhancer[34] showed lower accessibility in *Tet2-Tet3* DKO *i*NKT cells than in wild-type *i*NKT cells (Supplementary Fig. 7b). Other genes encoding cytokines and transcriptional regulators, such as *Il4*, *Ifng*, *Bcl11b* and *Satb1*, also showed downregulated expression, parallel loss of chromatin accessibility and gain of DNA modification, and this was sometimes, but not always, at the same genomic sites (Supplementary Fig. 8 and data not shown). There were also examples in which a substantial increase in DNA modification was observed without a corresponding decrease in gene expression (for example, *Gata3*; data not shown). Overall, the data points to a stronger link between chromatin accessibility and 5hmC (measured by CMS-IP) than between chromatin accessibility and DNA modification (5mC+5hmC; measured by WGBS).

Notably, of the 3,162 regions that showed greater chromatin accessibility in *Tet2-Tet3* DKO *i*NKT cells than in wild-type cells, eight were located in the vicinity of *Rorc* (Supplementary Fig. 7c), which correlated with higher expression of *Rorc* mRNA in *Tet2-Tet3* DKO *i*NKT cells than in wild-type *i*NKT cells (Supplementary Fig. 7c). One of these more-accessible regions, located upstream of the *Rorc* promoter, overlapped a predicted thymic-specific enhancer[34] (Supplementary Fig. 7c). Furthermore, motif-enrichment analysis of the 3,162 DARs that were more accessible in *Tet2-Tet3* DKO *i*NKT cells than in wild-type *i*NKT cells revealed considerable enrichment for the consensus RORγt-binding sequence (Fig. 7c); conversely, the 2,711 DARs that were less accessible in *Tet2-Tet3* DKO *i*NKT cells than in wild-type *i*NKT cells showed enrichment for consensus binding sequences for T-box- and basic-region-leucine (bZIP) transcription factors (Fig. 7c). Overall, the skewing toward the NKT17 cell lineage that we observed in *Tet2-Tet3* DKO *i*NKT cells might be explained by a combination of greater chromatin accessibility at the *Rorc* promoter and gene body and the enrichment for RORγt-binding motifs and loss of T-bet-binding motifs in *Tet2-Tet3* DKO *i*NKT cells relative to such features in wild-type *i*NKT cells.

Suppression of aberrant RORγt expression by ThPOK and T-bet

Unlike *Tbx21* (which encodes T-bet) and *Zbtb7b* (which encodes ThPOK), which both had high expression in wild-type *i*NKT cells and contained large amounts of 5hmC (Fig. 5b), *Rorc* had low expression and small amounts of 5hmC (Fig. 5b). T-bet and ThPOK probably both repress RORγt expression: T-bet deficiency redirects the development of *i*NKT cells toward the NKT2 and NKT17 cell lineages[6,40], and decreased expression of ThPOK

correlates with increased NKT17 differentiation[41]. To confirm that ThPOK and T-bet were able to suppress the aberrant overexpression of RORγt in *Tet2-Tet3* DKO *i*NKT cells, we retrovirally expressed these transcription factors in *Tet2-Tet3* DKO *i*NKT cells. Indeed, ThPOK, in the absence of TET2 and TET3, was sufficient to completely suppress RORγt expression (Fig. 8a,b) and IL-17 production (Fig. 8c). T-bet, on the other hand, only partially suppressed RORγt expression in *Tet2-Tet3* DKO *i*NKT cells (Fig. 8d,e). We concluded that the decrease in ThPOK and T-bet expression in *Tet2-Tet3* DKO *i*NKT cells might explain the increase in RORγt expression.

DISCUSSION

We studied mice with disrupted *Tet2* and *Tet3* genes at the DP stage of thymocyte development. *Tet2-Tet3* DKO mice showed a marked disease phenotype that reflected multiple factors: compromised development, migration and function of several T cell subsets; uncontrolled expansion of NKT17-cell-lineage-skewed *i*NKT cells; the appearance of innate $CD8^+$ cells that did not migrate to the periphery; and a dysfunctional phenotype of T_{reg} cells, with unstable Foxp3 expression resulting from impaired demethylation of the intronic *Foxp3* enhancer CNS2 (ref. 27). For all these disease features, loss of function of the TET proteins was necessary; individual deletion of TET2 or TET3 had only mild effects.

The phenotype of *i*NKT cell expansion was already apparent in 3-week-old mice that had not yet developed the disease phenotype; it was recapitulated by the transfer of small numbers of highly purified *Tet2-Tet3* DKO *i*NKT cells into immunocompetent recipient mice, which indicated that the expansion was not a result of the defect in functional T_{reg} cells in *Tet2-Tet3* DKO mice[27]. The expansion was antigen driven, as it was barely observed in CD1d-deficient recipient mice. T_{reg} cells and *i*NKT cells were the two cell types most affected in *Tet2-Tet3* DKO mice; a likely explanation is that conventional self-reactive T cells were deleted in the periphery, whereas both T_{reg} cells and *i*NKT cells were 'agonist selected' and thus proliferated and survived[42]. The dominant *i*NKT cell phenotype might also reflect the highly proliferative nature of developing *i*NKT cells[3]. *i*NKT cell expansion is also common in mice lacking other epigenetic regulators, such as Ezh2 (ref. 43) and Jarid2 (ref. 44), in T cells.

Notably, mice lacking individual TET proteins in T cells and hematopoietic stem cells show relatively mildly altered organismal phenotypes, such as individual germline deletions[45]. Deletions of *Tet1* and *Tet2* predispose mice to late-onset B cell malignancies and myeloid malignancies, respectively[45]. TET2 modulates cytokine production and gene expression in $CD4^+$ helper T cells[46] and partially controls T_{reg} cell function[27,47]. However, inducible deletion of both *Tet2* and *Tet3* in mouse hematopoietic stem cells is needed to cause the rapid development of an aggressive acute myeloid leukemia[35]. One possible explanation for this is that TET1 and TET2 have distinct functions, whereas TET2 and TET3 have more redundant roles. Indeed, TET1 has a major role in the deposition of 5hmC at promoter and TSS regions in mouse embryonic stem cells, whereas TET2 (and, as shown here, TET3) seems to act predominantly at distal enhancers[48]. Because of the lack of commercially available chromatin-immunoprecipitation-quality antibodies, we were not able to pinpoint the genomic regions at which TET2 and TET3 act in T cells.

Our genome-wide analyses provided a detailed view of the relationships among DNA-modification status (5mC+5hmC, assessed by WGBS), 5hmC distribution (assessed by CMS-IP), chromatin accessibility (assessed by ATAC-seq) and gene expression in thymic *i*NKT cells. These factors are interconnected: several transcription factors and chromatin modifiers have been shown to recruit TET proteins[45], and regions marked by 5hmC in wild-type *i*NKT cells showed more chromatin accessibility than that of *Tet2-Tet3* DKO *i*NKT cells. DMRs that lost or gained DNA modification (5mC+5hmC) during CLP–to–*i*NKT cell development also showed increased modification in *Tet2-Tet3* DKO *i*NKT cells, which indicated that TET proteins participate in developmental transitions in lymphoid-lineage cells. *Tbx21* and *Zbtb7b*, which encode the key transcriptional regulators T-bet and ThPOK, showed parallel decreases in 5hmC, chromatin accessibility and gene expression in *Tet2-Tet3* DKO *i*NKT cells relative to such features in wild-type *i*NKT cells, which indicated a requirement for TET2 and TET3. In contrast, the marked increase in accessibility and expression of *Rorc* and RORγt in *Tet2-Tet3* DKO *i*NKT cells appeared to be mediated indirectly through decreased expression of T-bet and ThPOK, as overexpression of either T-bet or ThPOK in *Tet2-Tet3* DKO *i*NKT cells suppressed RORγt expression. Future work will need to elucidate the precise sequence of molecular events that lead to TET-mediated control of *i*NKT cell expansion, lineage skewing and an acquisition of transmissible malignant phenotype.

ONLINE METHODS

Mice

Mice were housed in a pathogen-free animal facility at the La Jolla Institute for Allergy and Immunology and were used according to protocols approved by the Institutional Animal Care and Use Committee. *Tet2*$^{-/-}$ mice were generated by crossing CMVCre mice to *Tet2*$^{fl/fl}$ mice, in which exons 8, 9 and 10 that code for the catalytic HxD domain, were floxed (flanked by *lox*P sites)[15]. *Tet3*$^{fl/fl}$ mice were generated by targeting exon 2 (ref. 49). *Tet2*$^{-/-}$ and *Tet3*$^{fl/fl}$ mice were crossed with *Cd4-Cre*[50] mice to generate *Tet2*$^{-/-}$ *Tet3*$^{fl/fl}$ *Cd4-Cre* mice (DKO mice). These mice lack *Tet3* in the T cell lineage due to deletion of *Tet3* exon 2 in thymocytes at the CD4^{+}CD8^{+} (double-positive, DP) stage. The *Tet2-Tet3* DKO mice are in the C57BL/6 background. B6.SJL-PtprcaPep3bBoyJ (CD45.1^{+}) mice, C57BL/6 (CD45.2^{+}) mice and CD1dKO (*Cd1d*tg1.2) mice (B6(C)-*Cd1d1tm1.2Aben*/J) were purchased from Jackson laboratory. Both male and female mice were used in this study with similar findings. The majority of the experiments was done using young mice (3–5 weeks old as indicated). Analysis of older mice (6–8 weeks old) was performed to evaluate the lethal and aggressive nature of the observed phenotype. For transfer experiments 5–6 weeks old recipients were used. The recipients were of the same sex as the donors. Both male and female recipients were used and similar results were obtained.

Histology

Organs were isolated from age- and sex-matched control and *Tet2-Tet3* DKO mice and placed immediately in 10% formalin (Fisher), fixed overnight and then placed in 70% ethanol. Samples were paraffin-embedded, sectioned, stained with haematoxylin and eosin, and imaged using a Nikon Eclipse 80i microscope.

Flow Cytometry

Cells were isolated from thymus, spleen, lymph nodes and bone marrow. Surface staining was performed using antibodies from BioLegend: CD4 (RM4-5), CD8 (53-6.7), TCRβ (H57-597), B220 (RA3-6B2), CD44 (IM7), CD122 (5H4), CD24 (M1/69), CXCR3 (CXCR3-173), CD45.1 (A20), CD45.2 (104), CCR6 (29-2L17), CD103 (2E7), IL-4 (11B11), IL-17-F (9D3.1C8) and eBioscience: Eomes (Dan11mag), CD27 (LG-7F9) and IFN-γ (XMG1.2). PLZF (R17-809), T-bet (O4-46) and RORγt (Q31-378) were purchased from BD Pharmingen. In the initial stages of this study PLZF-Alexa Fluor 647 (D-9) was used and was obtained from Santa Cruz. α-GalCer–CD1d tetramer (conjugated either with PE or with BV421) was obtained from the NIH Tetramer Core. $V_α14$ *i*NKT cells were routinely defined as TCRβ intermediate, $B220^{-}$ and positive for α-GalCer–CD1d tetramer binding. Intracellular staining for transcription factors PLZF, RORγt and Eomes was performed using the Foxp3 staining kit (cat no: 00-5523-00) from eBioscience. In order to evaluate the simultaneous expression of PLZF and T-bet in *i*NKT cell subsets a different staining strategy was followed that in our hands significantly increased the efficiency of T-bet staining[51]. Briefly, cells were surfaced stained, washed in flow cytometry staining buffer (PBS containing 3% FBS), resuspended in 100 μl PBS and then add 100 μl of 4% methanol-free formaldehyde (Pierce) to obtain a final concentration of 2% formaldehyde. Cells were fixed for 30 min, centrifuged and washed in 200 μl of 1× permeabilization buffer from the Foxp3 staining kit (cat no: 00-5523-00) from eBioscience. Subsequently, the cells were resuspended in 1x Permeabilization buffer (Foxp3 staining kit) containing PLZF-A647 (R17-809) and T-bet (O4-46) Alexa Fluor 488 and RORγt (Q31-378) PE CF594. Acquisition was performed in a BD LSR Fortessa (BD Biosciences) using the BD FACSDiva Software. Data analysis was performed with FlowJo (Treestar).

Ex vivo cytokine production

Thymocytes (in a concentration of 1×10^6 cells/ml) were stimulated in the presence of 50 ng/ml PMA and 1.5 μM ionomycin for 4 h. In the last 2 h of culture Brefeldin A was added in a concentration of 10 μg/ml. Cells were washed, stained for surface markers and fixed with 2% of formaldehyde for 15 min at 37 °C. Subsequently the protocol of the transcription factor staining set from BD was followed to stain for IL-4 (11B11), IL17-F (9D3.1C8) and IFN-γ (XMG1.2).

In vivo BrdU incorporation

Mice were intraperitoneally injected with 100 μl of 10 mg/ml BrdU. 16 h later mice were euthanized and the cells were stained for surface markers and subsequently for BrdU according to the accompanying protocol (BD Pharmingen, APC BrdU flow kit 552598).

Isolation of $V_α14$ *i*NKT cells

$V_α14$ *i*NKT cell preparations for RNASeq analysis, CMS-IP seq and WGBS seq were performed using in case of control mice a pool of cells (isolated from thymus or spleen as indicated on each case) from C57BL/6 mice and from age- and sex-matched *Tet2-Tet3* DKO mice. For fluorescence-activated cell sorting (FACS), cells from wild-type mice were depleted of $CD19^{+}$ (6D5), TER-119^{+} (TER119), $CD8^{+}$ (53-6.7), $CD11c^{+}$ (N418), $F4/80^{+}$

(BM8) and CD11b$^+$ (M1/70) cells using biotinylated antibodies (BioLegend) and subsequent binding to magnetic streptavidin beads (Life Technologies). The unbound cells were incubated with 1 μg/ml Streptavidin A (Sigma-Aldrich) and subsequently stained with α-GalCer-loaded Cd1d tetramers and anti-TCRβ, after which tetramer-binding, TCRβ$^+$ cells were isolated using a FACSAria cell sorter (BD Biosciences). To obtain *Tet2-Tet3* DKO cells, no depletion was performed since *i*NKT cells had proliferated extensively. Rather, live B220$^-$ α-GalCer-Cd1d tetramer-binding, TCRβ$^+$ cells were isolated using a FACSAria cell sorter (BD Biosciences).

Transduction of Vα14 *Tet2-Tet3* DKO *i*NKT cells

3×10^6 PLAT-E cells were seeded in 10-cm plates. The cells were cultured in DMEM (Invitrogen) containing 10% FBS and in the absence of antibiotics. Retrovirus was produced by transfecting PLAT-E cells with pRV T-bet[52] or pMX-ThPOK-IRES-GFP. The Mirus transfection reagent was used according to the manufacturer's guidelines. We collected the supernatants 48 h and 72 h post-transfection and stored them at 4 °C. *i*NKT cells were sorted from *Tet2-Tet3* DKO mice 3–4 week-old and cultured in the presence of 10 ng/ml IL-7. 24 h and 48 h post sorting *i*NKT cells were infected by addition of virus in the presence of 10 μg/mL polybrene and centrifuged at 931 g for 90 min at 35 °C. 24 h after the second transduction *Tet2-Tet3* DKO *i*NKT cells were sorted based on GFP expression to separate un-transduced from transduced cells. To monitor if ThPOK and T-bet could bypass the loss of TET2 and TET3 and directly regulate RORγt expression and subsequent IL-17 secretion, GFP$^-$ (non-transduced) and GFP$^+$ (transduced) cells were compared by flow cytometry for RORγt expression. Cells were rested post sorting and restimulated in the presence of 10 nM of PMA and 1nM ionomycin for 4 h. 5 μg/ml brefeldin A (Sigma) was added for the last 2 h to inhibit cytokine secretion.

Splenocyte and *i*NKT cell adoptive transfer

Total splenocytes or sorted *i*NKT cells were transferred retro-orbitrally to non-irradiated, fully immune-competent congenic (B6.SJL-PtprcaPep3bBoyJ) (CD45.1$^+$) mice. The mice were monitored by bleeding and subsequent flow cytometry analysis to evaluate the proliferation of the transferred cells.

Bulk RNA-seq

Total RNA was isolated from thymic *i*NKT cells isolated from young (3–4 weeks old) mice and spleens from wild type or congenic recipients of *Tet2-Tet3* DKO *i*NKT cells using the E.Z.N.A. HP Total RNA kit (Omega) according to the manufacturer's instructions. Libraries were prepared using the Truseq RNA stranded kit (Illumina). The starting RNA material was 1 μg. Briefly, polyA$^+$ RNAs were selected with magnetic beads, the RNA was fragmented and cDNA was synthesized. After A-tailing and adaptor ligation, libraries were generated by amplifying the cDNA for 10–12 cycles. 3 different biological replicates per genotype were evaluated. The results of these experiments are shown in Figures 3a and 4d–f.

Micro-scaled RNA-seq (Smart-seq) of total *i*NKT cells

In this case, the starting total RNA for each library was 10 ng. RNA was isolated from wild-type, *Tet3 KO* and *Tet2-Tet3* DKO *i*NKT cells (data depicted in Fig. 3b) we performed SMART-seq as previously described[53]. RNA was isolated using the RNeasy Micro kit (Qiagen). RNA was incubated with free dNTPs and tailed oligo-dT oligonucleotides. The reverse transcription reaction was performed at 42 °C in the presence of 1 M betaine (Sigma) and increased concentration of $MgCl_2$ (6 mM) to increase cDNA yield. SuperScript II reverse transcriptase and RNAse Out Inhibitor (Invitrogen) were used. Template switching oligonucleotides (TSO) were added to enable template switching by the reverse transcriptase, which synthesizes a complementary sequence to the TSO. Nine cycles of pre-amplification were performed using the KAPA HiFi HotStart Ready Mix (Kapa Biosystems). PCR products were purified with Ampure XP beads (Beckman Coulter) and quantified using High Sensitivity DNA Qubit (Life Technologies). The size distribution of the amplified DNA was evaluated in a high-sensitivity Bioanalyzer DNA chip (Agilent). Following the pre-amplification step, cDNA was tagmented using Nextera XT DNA kit (Illumina). 1 ng of cDNA per tagmentation reaction was used. The reaction was performed at 55 °C for 5 min. The Tn5 tranposase was stripped off the tagmented DNA by adding neutralize tagment (NT) buffer according to the manufacturers. Eight cycles were performed for amplification of adaptor-ligated fragments using the Nextera PCR master mix and selected indexed primers (Nextera XT Index kit, Illumina). Two independent SMARTseq samples per genotype were used.

Micro-scaled RNA-seq (Smart-seq) of *i*NKT cell subsets

To prepare the SMART-seq samples for the wild-type and the *Tet2-Tet3* DKO subsets *i*NKT cell stage 1 (defined as TCR^{int} $tetramer^+$ $CD24^-NK1.1^+CD27^+CCR6^-$) ($n = 2$ subsets isolated from two different mice/genotype were assessed) and the TCR^{int} $tetramer^+$ $CD24^-NK1.1^-$ (containing mainly stage II *i*NKT cells) ($n = 3$ subsets isolated from three independent mice per genotype were evaluated). For the library preparation, ten cycles of PCR amplification were used. The data are shown in Figure 3c.

In all cases, the integrity of the isolated RNA was evaluated in the Bioanalyzer (Agilent Technologies). Only samples with a minimum RIN value of 9 were used for library preparation. The quality and quantity of the amplified libraries was evaluated using Bioanalyzer (Agilent Technologies Inc) and HS Qubit (Life Technologies). The libraries were pooled in a concentration of 10 nM and sequenced using an Illumina Hiseq 2500 instrument.

Genome-wide 5hmC mapping by CMS-IP-seq

$V_\alpha 14$ *i*NKT cells were isolated by flow cytometry and DNA was isolated using the PureLink genomic DNA mini kit (Life Technologies). DNA was fragmented to an average size of 200 bp using the Adaptive Focused Acoustics Covaris S2 instrument. Library preparation, bisulfite treatment and immunoprecipitation of CMS (5hmC)-enriched DNA were performed as previously described[13,31]. Briefly, fully unmethylated λ (lambda) DNA (Promega) was spiked into the mouse genomic DNA at a ratio of 1:200. DNA was end-repaired using the End Repair (Illumina Epicentre) and A-tailed (using Klenow fragment, New England

BioLabs). Ligation of methylated adapters (NeBNext Multiplex Oligos for Illumina, New England BioLabs) was performed using Quick Ligase Kit (New England BioLabs). DNA was bisulfite-treated using the MethylCode Bisulfite Conversion Kit (Life Technologies). 1% of bisulfite-converted DNA was kept as input and the rest was used for immunoprecipitation with anti-CMS antibody[31]. The anti-CMS recognizes 5hmC that upon bisulfite treatment is converted to cytosine-5-methylenesulfonate (CMS), enabling thus the enrichment of 5hmC containing DNA fragments[31]. The immunoprecipitated DNA was amplified using Kapa HiFi Uracil$^+$ (Kapa Biosystems). Two different CMS-IP samples per genotype were evaluated.

Whole-genome bisulfite sequencing (WGBS-seq)

$V_\alpha 14$ *i*NKT cells were isolated by flow cytometry and DNA was isolated using the PureLink genomic DNA mini kit (Life technologies). DNA was fragmented. 1.5 μg of the fragmented DNA was used for the library preparation and bisulfite treatment was done as described in the CMS-IP seq section. After the bisulfite conversion the purified DNA was amplified for 4 cycles (low amplification) using Kapa HiFi Uracil$^+$ (Kapa Biosystems). 2 independent WGBS samples per genotype were evaluated.

In describing the WGBS data, we use the term “DNA modification” (5mC+5hmC) in preference to “DNA methylation” because bisulfite sequencing does not distinguish between 5mC and 5hmC[54], and because dot blot analysis shows persisting 5hmC in *Tet2-Tet3* DKO thymocytes (Supplementary Fig. 1b) that is most likely deposited by TET1 (Supplementary Fig. 1a). However, the term “DNA methylation” is approximately correct, since 5hmC represents only a small percentage of total modified cytosines in T cells (<10% of 5mC)[14,55].

To examine changes in DNA modification at the level of individual TSS regions and gene bodies, we calculated the average change in DNA modification in each gene body and at each promoter/TSS region (DMR discovery; Supplementary Methods), and plotted the values against the change in expression of the corresponding gene (Supplementary Fig. 6b).

Identifying chromatin accessibility by the assay of transposase-accessible chromatin sequencing (ATAC-seq)

Libraries were prepared as previously described[38]. 5×10^4 *i*NKT cells were sorted, washed once with PBS and lysed in 100 μl of ice-cold lysis buffer (10 mM Tris-HCl, pH 7.4, 10 mM NaCl, 3 mM $MgCl_2$ and 0.1% IGEPAL CA-630). Then, nuclei were spun at 500*g* for 10 min and the pellet was resuspended in 50 μl transposase reaction mix [2.5 μl transposase (Illumina), 25 μl 2 × TD buffer (Illumina) and 22.5 μl nuclease free water). The reaction was incubated for 30 min at 37 °C. Samples were purified using MinElute kit (Qiagen). The purified DNA was amplified using Kapa Real time library amplification kit (Kapa Biosystems). Libraries were amplified for 10–11 cycles. *i*NKT cells isolated from 3 different mice/genotype were evaluated.

Quantitative real-time RT PCR

Total RNA from DP, CD4SP and CD8SP T cells was isolated with E.Z.N.A HP Total RNA. cDNA was synthesized using Superscript reverse transcriptase and oligo(dT) primers (Life Techologies), and gene expression was evaluated with Step One Plus (Applied Biosystems) using Roche SYBR green real-time master. The following primers were used: Tet1F: 5′-GAGCCTGTTCCTCGATGTGG-3′, Tet1R: 5′-CAAACCCACCTGAGGCTGTT-3′, Tet2F: 5′-AACCTGGCTACTGTCATTGCTCCA-3′, Tet2R: 5′-ATGTTCTGCTGGTCTCTGTGGGAA-3′; Tet3F: 5′-GTCT CCCCAGTCCTACCTCCG-3′, Tet3R: 5′-GTCAGTGCCCCACGCTTCA-3′

Analysis of CMS (bisulfite-converted 5hmC) abundance by dot blot

100 ng genomic DNA samples were sheared using needle and treated with sodium bisulfite using the Methylcode bisulfite kit (Invitrogen). DNA was prepared using twofold serial dilutions in TE buffer and then denatured in 0.4 M NaOH, 10mM EDTA at 95 °C for 10 min and followed by adding an equal volume of cold 2M ammonium acetate (pH 7.0) on ice for 10 min. Denatured DNA samples were spotted on a nitrocellulose membrane in an assembled Bio-Dot apparatus (Bio-Rad) according to the manufacturer's instructions. The membrane was washed with 2 × SSC buffer and then vacuum-baked at 80 °C for 2 h. Then the membrane was blocked with 5% non-fat milk for 1 h and incubated with rabbit antisera against CMS detected by HRP conjugated secondary antibody and enhanced chemiluminescence.

Statistical Analysis

Statistical analysis was performed with GraphPAd Prism6 (Graphpad software). Unpaired *t* test, Log-rank (Mantel-Cox) test and Gehan-Brenslow-Wilcoxon test were applied as indicated and the *P*-values are shown for each figure. Data are mean ± s.e.m. If not otherwise indicated the *P* value was not statistically significant ($P > 0.05$). In the graphs each dot represents a mouse. For all the experiments we used sufficient number of mice to ensure adequate power for our conclusions. Mice from different litters and of different sex were evaluated. In addition, we ensured that a minimum of 2 independent experiments was performed in each case. No blinding was applied in this study.

Data availability

Data that support the findings of this study have been deposited in GEO with the accession code GSE66834. Source data for Figures 3–7 are provided with the paper.

Supplementary Material

Refer to Web version on PubMed Central for supplementary material.

Acknowledgments

We thank C. Kim, K. van Gunst, L. Nosworthy, D. Hinz and R. Simmons at the LJI Flow Cytometry Core for help with fluorescence-activated cell sorting; G. Seumois and J. Day at the LJI Functional Genomics Center for assistance with next-generation sequencing (Illumina HiSeq 2500); M. Kronenberg, I. Engel and C.-W. Lio (LJI) for discussions, the LJI Bioinformatics Core for routine analysis; Z. Mikulski and B. Kiosses at the LJI microscopy core, M. Chadwell at the LJI Histology core, and the Histology Core at the University of California at San Diego

Moores Cancer Center; and R. Bosselut (National Cancer Institute) for pMX-ThPOK-IRES-GFP. Supported by US National Institutes of Health (R01 AI44432, CA151535 and R35CA210043), the Leukemia and Lymphoma Society (Translation Research Project grant 6187-12 to A.R.), the Academy of Finland Centre of Excellence in Molecular Systems Immunology and Physiology Research (H.L. and. S.R.), an Albert Billings Ruddock Professorship at Caltech (E.V.R.), the Cancer Research Institute (Irvington Institute postdoctoral fellowship to A.T.), the Fraternal Order of Eagles Fellow of the Damon Runyon Cancer Research Foundation (DRG-2069-11 to J.P.S.-B.) and the National Science Foundation (W.A.P.).

References

1. Yui MA, Rothenberg EV. Developmental gene networks: a triathlon on the course to T cell identity. Nat Rev Immunol. 2014; 14:529–545. [PubMed: 25060579]
2. Carpenter AC, Bosselut R. Decision checkpoints in the thymus. Nat Immunol. 2010; 11:666–673. [PubMed: 20644572]
3. Bendelac A, Savage PB, Teyton L. The biology of NKT cells. Annu Rev Immunol. 2007; 25:297–336. [PubMed: 17150027]
4. Vahedi G, et al. Helper T-cell identity and evolution of differential transcriptomes and epigenomes. Immunol Rev. 2013; 252:24–40. [PubMed: 23405893]
5. Hogquist KA, Jameson SC. The self-obsession of T cells: how TCR signaling thresholds affect fate 'decisions' and effector function. Nat Immunol. 2014; 15:815–823. [PubMed: 25137456]
6. Lee YJ, Holzapfel KL, Zhu J, Jameson SC, Hogquist KA. Steady-state production of IL-4 modulates immunity in mouse strains and is determined by lineage diversity of *i*NKT cells. Nat Immunol. 2013; 14:1146–1154. [PubMed: 24097110]
7. Winter DR, Amit I. The role of chromatin dynamics in immune cell development. Immunol Rev. 2014; 261:9–22. [PubMed: 25123274]
8. Smith ZD, Meissner A. DNA methylation: roles in mammalian development. Nat Rev Genet. 2013; 14:204–220. [PubMed: 23400093]
9. Tahiliani M, et al. Conversion of 5-methylcytosine to 5-hydroxymethylcytosine in mammalian DNA by MLL partner TET1. Science. 2009; 324:930–935. [PubMed: 19372391]
10. Ito S, et al. Tet proteins can convert 5-methylcytosine to 5-formylcytosine and 5-carboxylcytosine. Science. 2011; 333:1300–1303. [PubMed: 21778364]
11. He YF, et al. Tet-mediated formation of 5-carboxylcytosine and its excision by TDG in mammalian DNA. Science. 2011; 333:1303–1307. [PubMed: 21817016]
12. Pastor WA, Aravind L, Rao A. TETonic shift: biological roles of TET proteins in DNA demethylation and transcription. Nat Rev Mol Cell Biol. 2013; 14:341–356. [PubMed: 23698584]
13. Tsagaratou A, et al. Dissecting the dynamic changes of 5-hydroxymethylcytosine in T-cell development and differentiation. Proc Natl Acad Sci USA. 2014; 111:E3306–E3315. [PubMed: 25071199]
14. Ko M, et al. Impaired hydroxylation of 5-methylcytosine in myeloid cancers with mutant TET2. Nature. 2010; 468:839–843. [PubMed: 21057493]
15. Ko M, et al. Ten-Eleven-Translocation 2 (TET2) negatively regulates homeostasis and differentiation of hematopoietic stem cells in mice. Proc Natl Acad Sci USA. 2011; 108:14566–14571. [PubMed: 21873190]
16. Gu TP, et al. The role of Tet3 DNA dioxygenase in epigenetic reprogramming by oocytes. Nature. 2011; 477:606–610. [PubMed: 21892189]
17. Lee YJ, Jameson SC, Hogquist KA. Alternative memory in the CD8 T cell lineage. Trends Immunol. 2011; 32:50–56. [PubMed: 21288770]
18. Engel I, et al. Innate-like functions of natural killer T cell subsets result from highly divergent gene programs. Nat Immunol. 2016; 17:728–739. [PubMed: 27089380]
19. Yu S, et al. The TCF-1 and LEF-1 transcription factors have cooperative and opposing roles in T cell development and malignancy. Immunity. 2012; 37:813–826. [PubMed: 23103132]
20. Karo JM, Schatz DG, Sun JC. The RAG recombinase dictates functional heterogeneity and cellular fitness in natural killer cells. Cell. 2014; 159:94–107. [PubMed: 25259923]

21. Matthews JM, Lester K, Joseph S, Curtis DJ. LIM-domain-only proteins in cancer. Nat Rev Cancer. 2013; 13:111–122. [PubMed: 23303138]
22. Ramsay RG, Gonda TJ. MYB function in normal and cancer cells. Nat Rev Cancer. 2008; 8:523–534. [PubMed: 18574464]
23. Uddin MN, et al. Transcription factor Bcl11b sustains iNKT1 and iNKT2 cell programs, restricts iNKT17 cell program, and governs iNKT cell survival. Proc Natl Acad Sci USA. 2016; 113:7608–7613. [PubMed: 27330109]
24. Mathew R, et al. BTB-ZF factors recruit the E3 ligase cullin 3 to regulate lymphoid effector programs. Nature. 2012; 491:618–621. [PubMed: 23086144]
25. Dose M, et al. Intrathymic proliferation wave essential for Valpha14^{+} natural killer T cell development depends on c-Myc. Proc Natl Acad Sci USA. 2009; 106:8641–8646. [PubMed: 19423665]
26. Carr T, et al. The transcription factor lymphoid enhancer factor 1 controls invariant natural killer T cell expansion and T_H2-type effector differentiation. J Exp Med. 2015; 212:793–807. [PubMed: 25897173]
27. Yue X, et al. Control of Foxp3 stability through modulation of TET activity. J Exp Med. 2016; 213:377–397. [PubMed: 26903244]
28. Wolf E, Lin CY, Eilers M, Levens DL. Taming of the beast: shaping Myc-dependent amplification. Trends Cell Biol. 2014; 25:241–248. [PubMed: 25475704]
29. Lee YJ, et al. Lineage-specific effector signatures of invariant NKT cells are shared amongst γδ T, innate lymphoid, and T_H cells. J Immunol. 2016; 197:1460–1470. [PubMed: 27385777]
30. Fonseca-Pereira D, et al. The neurotrophic factor receptor RET drives haematopoietic stem cell survival and function. Nature. 2014; 514:98–101. [PubMed: 25079320]
31. Huang Y, Pastor WA, Zepeda-Martínez JA, Rao A. The anti-CMS technique for genome-wide mapping of 5-hydroxymethylcytosine. Nat Protoc. 2012; 7:1897–1908. [PubMed: 23018193]
32. Pastor WA, et al. Genome-wide mapping of 5-hydroxymethylcytosine in embryonic stem cells. Nature. 2011; 473:394–397. [PubMed: 21552279]
33. Laurent L, et al. Dynamic changes in the human methylome during differentiation. Genome Res. 2010; 20:320–331. [PubMed: 20133333]
34. Shen Y, et al. A map of the cis-regulatory sequences in the mouse genome. Nature. 2012; 488:116–120. [PubMed: 22763441]
35. An J, et al. Acute loss of TET function results in aggressive myeloid cancer in mice. Nat Commun. 2015; 6:10071. [PubMed: 26607761]
36. Kieffer-Kwon KR, et al. Interactome maps of mouse gene regulatory domains reveal basic principles of transcriptional regulation. Cell. 2013; 155:1507–1520. [PubMed: 24360274]
37. Lara-Astiaso D, et al. Immunogenetics. chromatin state dynamics during blood formation. Science. 2014; 345:943–949. [PubMed: 25103404]
38. Buenrostro JD, Giresi PG, Zaba LC, Chang HY, Greenleaf WJ. Transposition of native chromatin for fast and sensitive epigenomic profiling of open chromatin, DNA-binding proteins and nucleosome position. Nat Methods. 2013; 10:1213–1218. [PubMed: 24097267]
39. Jeong M, et al. Large conserved domains of low DNA methylation maintained by Dnmt3a. Nat Genet. 2014; 46:17–23. [PubMed: 24270360]
40. Townsend MJ, et al. T-bet regulates the terminal maturation and homeostasis of NK and Valpha14i NKT cells. Immunity. 2004; 20:477–494. [PubMed: 15084276]
41. Engel I, Zhao M, Kappes D, Taniuchi I, Kronenberg M. The transcription factor Th-POK negatively regulates T_H17 differentiation in Vα14i NKT cells. Blood. 2012; 120:4524–4532. [PubMed: 23034280]
42. Stritesky GL, Jameson SC, Hogquist KA. Selection of self-reactive T cells in the thymus. Annu Rev Immunol. 2012; 30:95–114. [PubMed: 22149933]
43. Dobenecker MW, et al. Coupling of T cell receptor specificity to natural killer T cell development by bivalent histone H3 methylation. J Exp Med. 2015; 212:297–306. [PubMed: 25687282]
44. Pereira RM, et al. Jarid2 is induced by TCR signaling and controls iNKT cell maturation. Nat Commun. 2014; 5:4540. [PubMed: 25105474]

45. Rasmussen KD, Helin K. Role of TET enzymes in DNA methylation, development, and cancer. Genes Dev. 2016; 30:733–750. [PubMed: 27036965]
46. Ichiyama K, et al. The methylcytosine dioxygenase Tet2 promotes DNA demethylation and activation of cytokine gene expression in T cells. Immunity. 2015; 42:613–626. [PubMed: 25862091]
47. Sasidharan Nair V, Song MH, Oh KI. Vitamin C facilitates demethylation of the Foxp3 enhancer in a Tet-dependent manner. J Immunol. 2016; 196:2119–2131. [PubMed: 26826239]
48. Huang Y, et al. Distinct roles of the methylcytosine oxidases Tet1 and Tet2 in mouse embryonic stem cells. Proc Natl Acad Sci USA. 2014; 111:1361–1366. [PubMed: 24474761]
49. Ko M, et al. TET proteins and 5-methylcytosine oxidation in hematological cancers. Immunol Rev. 2015; 263:6–21. [PubMed: 25510268]
50. Lee PP, et al. A critical role for Dnmt1 and DNA methylation in T cell development, function, and survival. Immunity. 2001; 15:763–774. [PubMed: 11728338]
51. Heinen AP, et al. Improved method to retain cytosolic reporter protein fluorescence while staining for nuclear proteins. Cytometry A. 2014; 85:621–627. [PubMed: 24616430]
52. Djuretic IM, et al. Transcription factors T-bet and Runx3 cooperate to activate Ifng and silence Il4 in T helper type 1 cells. Nat Immunol. 2007; 8:145–153. [PubMed: 17195845]
53. Picelli S, et al. Full-length RNA-seq from single cells using Smart-seq2. Nat Protoc. 2014; 9:171–181. [PubMed: 24385147]
54. Huang Y, et al. The behaviour of 5-hydroxymethylcytosine in bisulfite sequencing. PLoS One. 2010; 5:e8888. [PubMed: 20126651]
55. Tsagaratou A, Rao A. TET proteins and 5-methylcytosine oxidation in the immune system. Cold Spring Harb Symp Quant Biol. 2013; 78:1–10. [PubMed: 24619230]

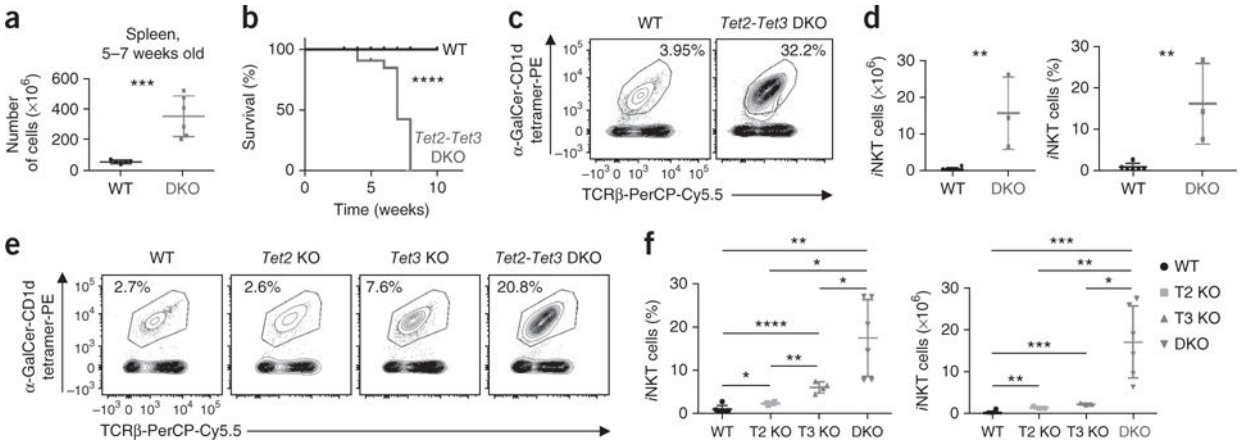

Figure 1.

Simultaneous deletion of *Tet2* and *Tet3* severely compromises T cell homeostasis, leading to *i*NKT cell expansion and disease. (**a**) Quantification of total cells in the spleen of 5- to 7-week-old wild-type mice (WT) ($n = 5$) and *Tet2-Tet3* DKO mice (DKO) ($n = 6$). (**b**) Disease-free survival of wild-type mice ($n = 10$) and *Tet2-Tet3* DKO mice ($n = 10$) (Kaplan-Meier curve). (**c**) *i*NKT cells in spleens of 4-week-old wild-type ($n = 6$) versus *Tet2-Tet3* DKO ($n = 3$) mice. (**d**) Quantification (left) and frequency (right) of *i*NKT cells in spleens isolated from 4-week-old *Tet2-Tet3* DKO mice ($n = 3$) and wild-type mice ($n = 6$). (**e**) *i*NKT cells in the spleen of 3- to 4-week-old wild-type mice ($n = 5$), *Tet2*$^{-/-}$ (*Tet2* KO) mice ($n = 3$), *Tet3* KO mice ($n = 3$) and *Tet2-Tet3* DKO mice ($n = 6$). (**f**) Frequency of *i*NKT cells in wild-type mice ($n = 5$), *Tet2* KO mice ($n = 3$), *Tet3* KO mice ($n = 4$) and *Tet2-Tet3* DKO mice ($n = 6$) (left), and number of *i*NKT cells in wild-type mice ($n = 3$), *Tet2* KO mice ($n = 3$), *Tet3* KO mice ($n = 3$) and *Tet2-Tet3* DKO mice ($n = 6$) (right). Numbers adjacent to outlined areas (**c**,**e**) indicate percent tetrameter+TCRβ$^+$ cells. Each symbol (**a**,**d**,**f**) represents an individual mouse; horizontal lines indicate the mean (± s.e.m.). *$P < 0.05$, **$P < 0.01$, ***$P < 0.001$ and ****$P < 0.0001$ (unpaired *t*-test). Data are representative of 5 experiments (**a**), 10 experiments (**b**), 3 experiments (**d**), 3 experiments (**e**) or 3 experiments (**f**) or are from three independent experiments (**c**).

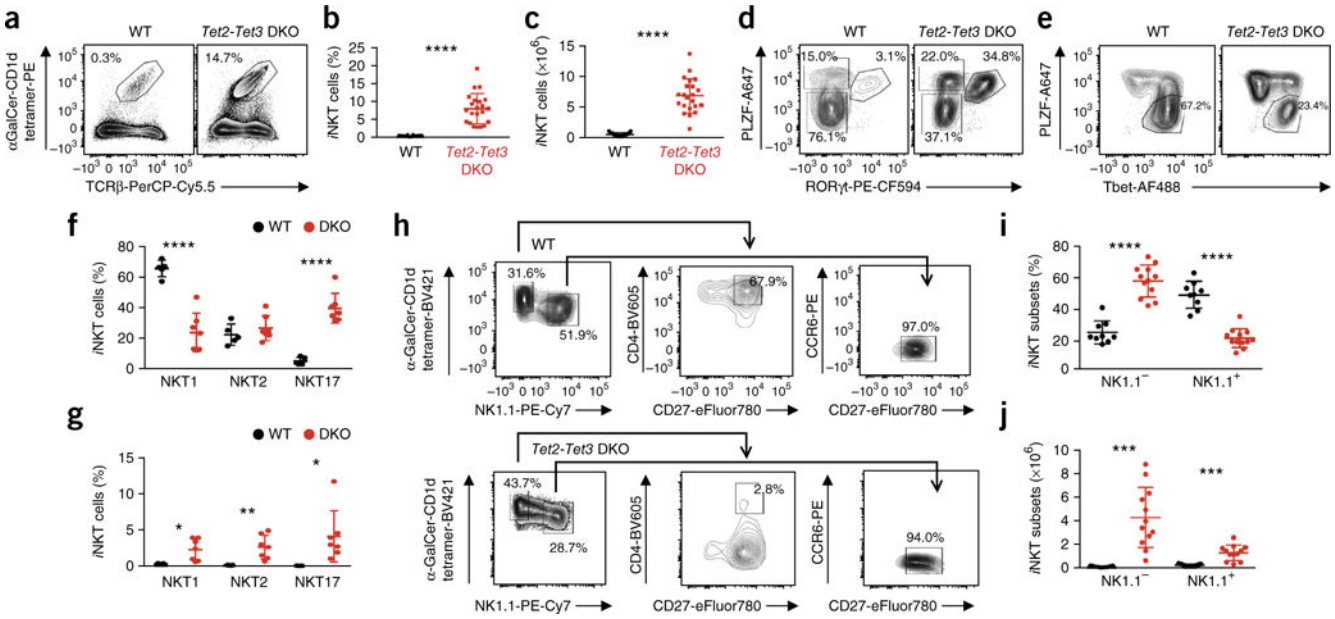

Figure 2.

Tet2-Tet3 DKO *i*NKT cells in the thymus of young (3- to 4-week-old) mice are skewed toward the NKT17 cell lineage. (**a**) *i*NKT cells in the thymus of 20-day-old wild-type and *Tet2-Tet3* DKO mice. Numbers adjacent to outlined areas indicate percent tetrameter +TCRβ$^+$ cells. (**b**,**c**) Frequency (**b**) and number (**c**) of *i*NKT cells in the thymus of *Tet2-Tet3* DKO mice ($n = 22$) and wild-type mice ($n = 15$). (**d**) Flow cytometry analysis of the expression of PLZF and RORγt in tetramer$^+$CD24$^-$TCRβ$^+$ thymocytes. (**d**,**e**) Flow cytometry analysis of the expression of PLZF and RORγt (**d**) or of PLZF and T-bet (**e**) in tetramer$^+$CD24$^-$TCRβ$^+$ thymocytes. (**f**) Frequency of *i*NKT cell subsets among total *i*NKT cells. (**g**) Results in **f**, presented as frequency among total thymocytes. (**h**) Flow cytometry of tetramer$^+$CD24$^-$TCRβ$^+$ thymocytes from wild-type mice ($n = 9$) (top) and *Tet2-Tet3* DKO mice ($n = 12$) (bottom), analyzing the expression of NK1.1 and binding of tetramer (left), expression of CD4 and CD27 in the tetramer$^+$NK1.1$^-$ subset (arrow) (middle), and expression of CCR6 and CD27 in the tetramer$^+$NK1.1$^+$ subset (arrow) (right). (**i**) Frequency of the NK1.1$^-$ and NK1.1$^+$ subsets (as defined in **h**) among total *i*NKT cells. (**j**) Quantification of the NK1.1$^-$ and NK1.1$^+$ subsets (as defined in **h**) among total *i*NKT cells. Numbers adjacent to outlined areas (**a**,**d**,**e**,**h**) indicate percent cells in each. Each symbol (**b**,**c**,**f**,**g**,**i**,**j**) represents an individual mouse; horizontal lines indicate the mean (± s.e.m.). *$P < 0.05$, **$P < 0.01$, ***$P < 0.001$ and ****$P < 0.0001$ (unpaired *t*-test). Data are representative of 15 experiments (**a**), 5 experiments (**i**), 5 experiments (**i**), are from one experiment representative of four experiments (**b**–**e**) or are from four independent experiments with five wild-type mice and seven *Tet2-Tet3* DKO mice (**f**,**g**) or five independent experiments (**h**).

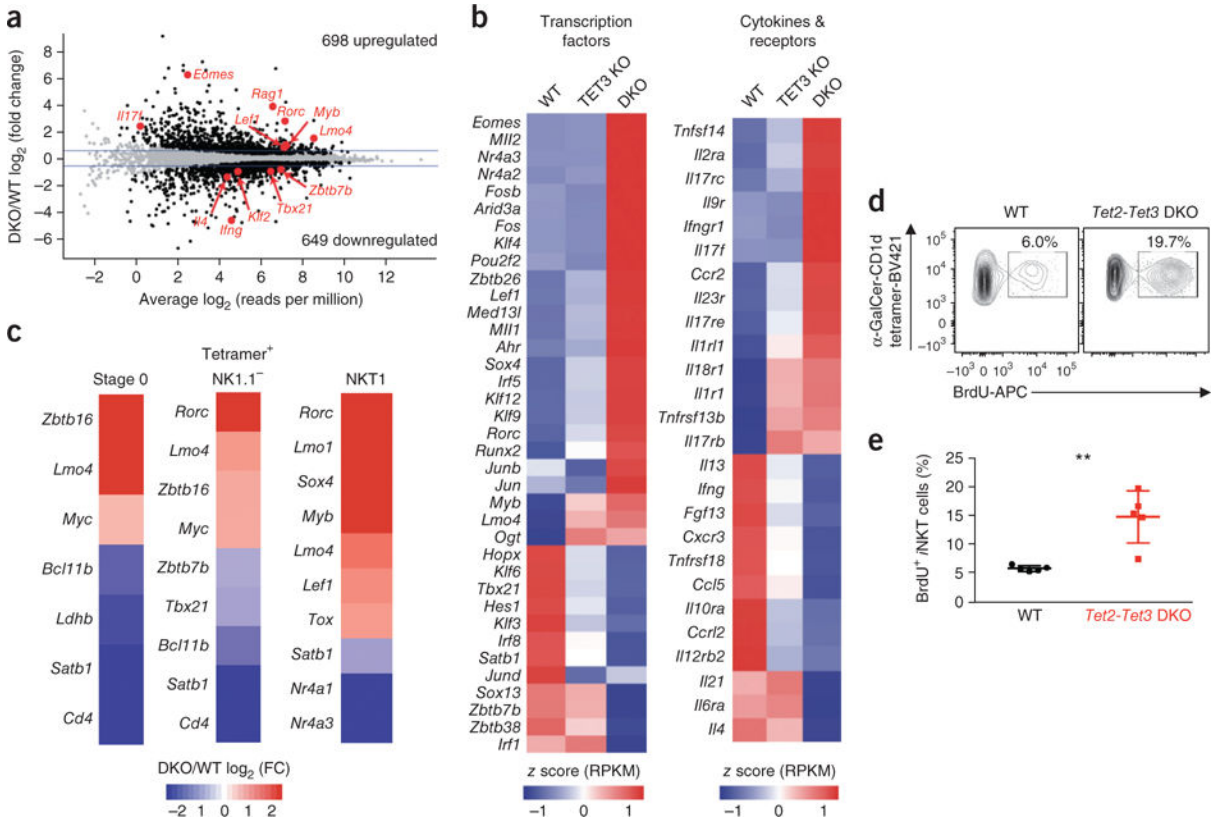

Figure 3.

Gene-expression profiles of thymic wild-type and *Tet2-Tet3* DKO *i*NKT cells. (**a**) Mean average (MA) plot of genes expressed differentially in thymic *i*NKT cells isolated from *Tet2-Tet3* DKO relative to their expression in such cells from wild-type mice. (**b**) Expression of genes encoding selected transcriptional regulators (left) and cytokines and their receptors (right) in *Tet2-Tet3* DKO, *Tet3* KO and wild-type thymic *i*NKT cells, presented as row-wise *z*-scores (red, higher expression, and blue, lower expression, relative to other conditions). (**c**) Expression of selected genes of interest in stage 0, NK1.1^{-} and NKT1 *i*NKT subsets. (**d**) Flow cytometry analysis of BrdU incorporation in tetramer^{+}TCRβ^{+} thymocytes. Numbers adjacent to outlined areas indicate percent cells with BrdU incorporation. (**e**) Frequency of tetramer^{+}TCRβ^{+} *i*NKT cells that incorporated BrdU. Each symbol represents an individual mouse; horizontal lines indicate the mean (± s.e.m.). $^{**}P < 0.01$, (unpaired *t* test). Data are representative of one experiment with three biological replicates per genotype (**a**), one experiment with two biological replicates per genotype (**b**), one experiment with two biological replicates per genotype for stage 0, three biological replicates per genotype for NK1.1^{-}, two biological replicates wild-type NKT1, and three biological replicates per genotype for DKO NKT1 (**c**), are from one experiment representative of two experiments with five mice per genotype (**d**) or from two independent experiments with five mice per genotype (**e**).

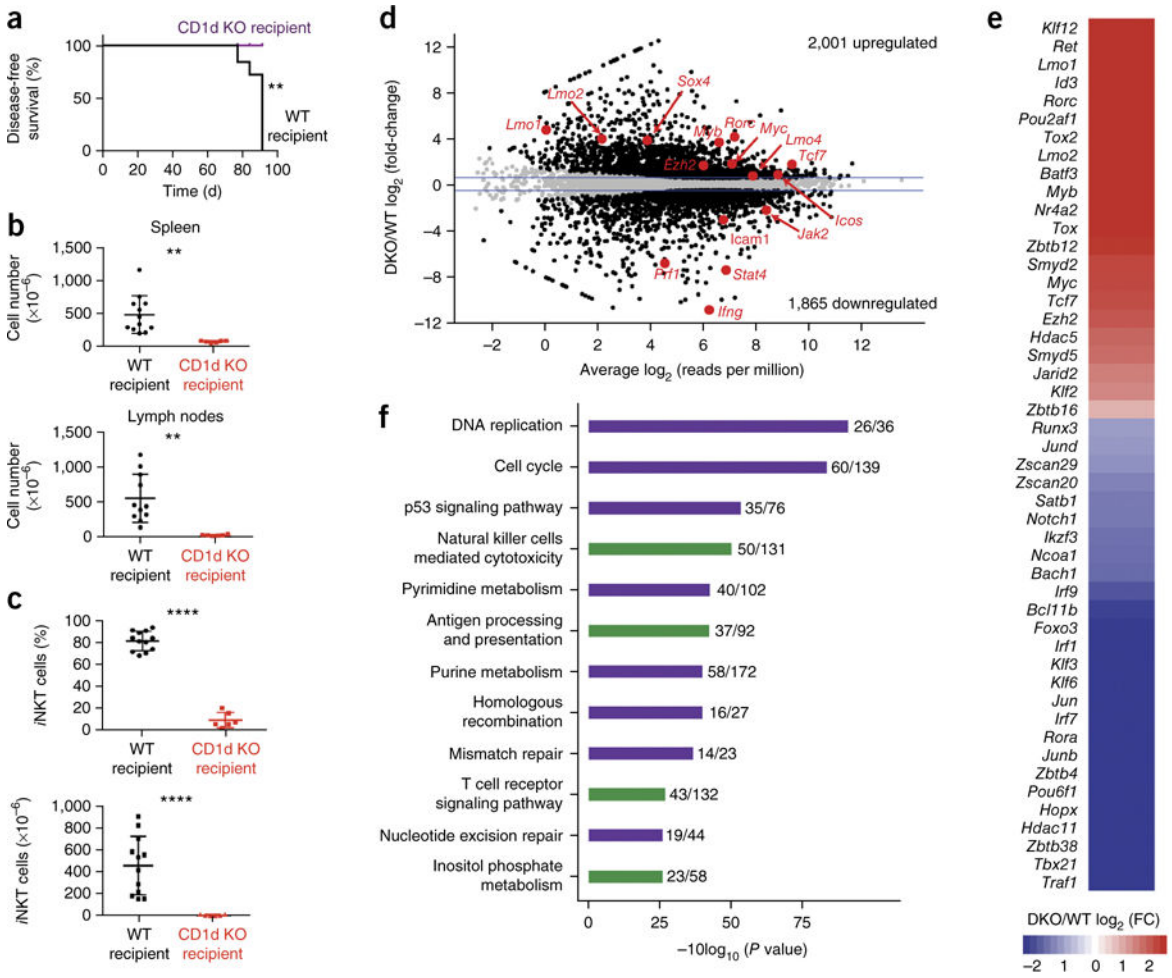

Figure 4.

Antigen stimulation promotes the expansion of *Tet2-Tet3* DKO *i*NKT cells and disease development in fully immunocompetent recipients. (**a**) Disease-free survival of wild-type (n = 6) and CD1dKO recipients (n = 5) of *Tet2-Tet3* DKO *i*NKT cells (Kaplan-Meier curve). $^{**}P < 0.01$ (log-rank (Mantel-Cox) test and Gehan-Brenslow-Wilcoxon test). (**b**) Cellularity of the spleen (left) and lymph nodes (right) of wild-type recipients (n = 12) and CD1dKO recipients (n = 6) of *Tet2-Tet3* DKO *i*NKT cells. (**c**) Frequency (top) and numbers (bottom) of *i*NKT cells in the spleen of wild-type recipients (n = 12) and CD1dKO recipients (n = 6) of *Tet2-Tet3* DKO *i*NKT cells. (**d**) MA plot of genes expressed differentially in transferred and expanded *Tet2-Tet3* DKO *i*NKT cells isolated from the spleen of congenic recipient mice relative to their expression in *i*NKT cells isolated from the spleen of healthy wild-type mice. (**e**) Expression ($\log_2$ fold values) of selected genes encoding transcriptional regulators with differential expression (higher (red) or lower (blue)) in *Tet2-Tet3* DKO *i*NKT cells than in wild-type *i*NKT cells. (**f**) Pathway-enrichment analysis of differentially expressed genes in transferred *Tet2-Tet3* DKO *i*NKT cells: purple, categories related to DNA replication, cell cycle and DNA repair; green, categories related to T cell function. Each symbol (**b**,**c**) represents an individual mouse; horizontal lines indicate the mean (± s.e.m.). $^{**}P < 0.01$, $^{***}P < 0.001$ (unpaired t test). Data are from two independent experiments (**a**), three

independent experiments (**b**,**c**), or one experiment with three biological replicates per genotype (**d**–**f**).

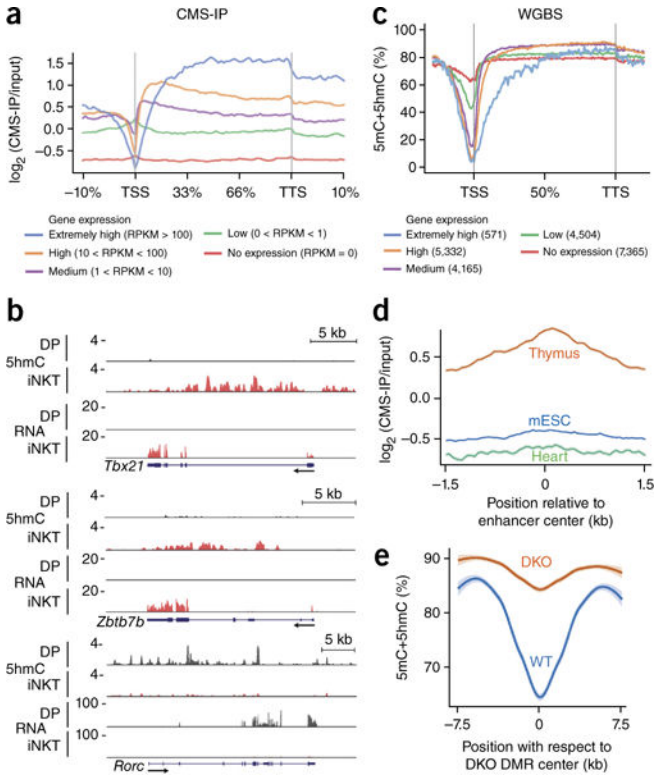

Figure 5.

5hmC shows enrichment in the bodies of genes with high expression in *i*NKT cells and those expressing key *i*NKT-cell-lineage-specifying factors. (**a**) CMS-IP analysis of the enrichment for 5hmC over the gene body, categorized on the basis of gene expression (RNA-seq analysis), in wild-type thymic *i*NKT cells. (**b**) Genome browser views of intragenic 5hmC (CMS-IP analysis) and gene expression (RNA-seq analysis) in *Tbx21*, *Zbtb7b* and *Rorc* in wild-type thymocytes. (**c**) Average enrichment for 5mC+5hmC over the gene body, categorized on the basis of gene expression (WGBS and RNA-seq analysis), in wild-type thymic *i*NKT cells. (**d**) Average enrichment of 5hmC in wild-type *i*NKT cells from tissue-specific enhancers in the thymus (orange), mouse embryonic stem cells (mESC; blue) and heart (green)[34]. (**e**) Modification of 5mC+5hmC in wild-type and *Tet2-Tet3* DKO *i*NKT cells, plotted against position relative to DMR. Data are representative of one experiment with two biological replicates for CMS-IP seq, two biological replicates for WGBS and three biological replicates for RNA-seq.

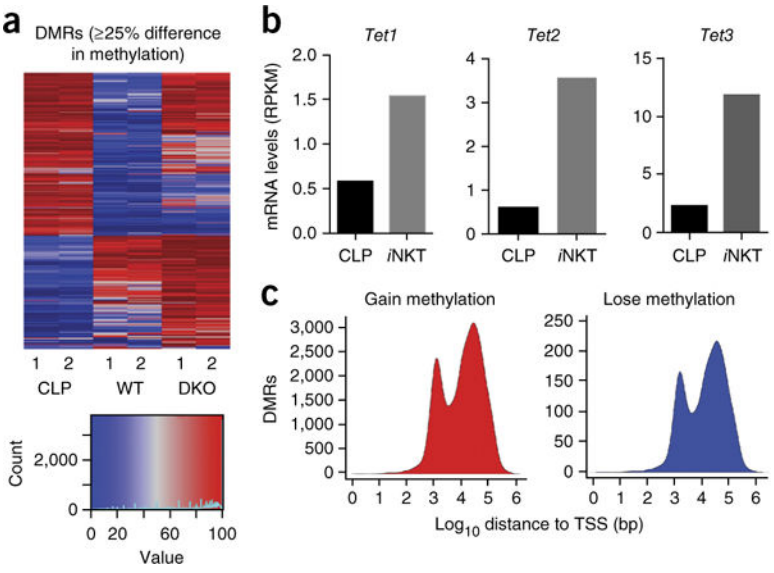

Figure 6.

TET proteins regulate DNA modification in *i*NKT cells. (**a**) DNA modification in CLPs and wild-type and *Tet2-Tet3* DKO *i*NKT cells, showing more (red) or less (blue) modification. (**b**) RNA-seq analysis of *Tet1*, *Tet2* and *Tet3* in *i*NKT cells and CLPs. (**c**) Quantification of DMRs relative to their distance to the TSS. Data are representative of one experiment with two technical replicates for CLPs and two biological replicates per genotype for *i*NKT cells (**a**,**c**), and three biological replicates for *i*NKT cells and one sample for CLPs (**b**).

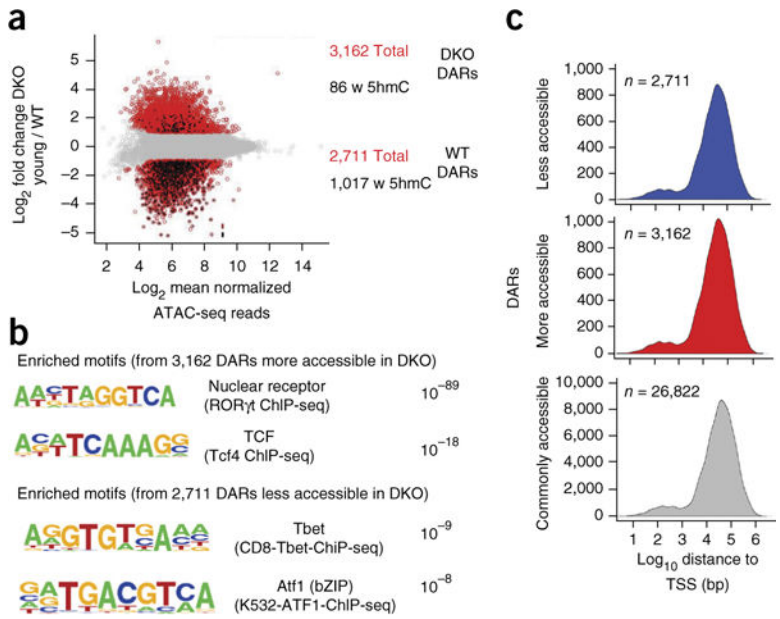

Figure 7.

Characterization of chromatin regions with differential accessibility in wild-type *i*NKT cells versus *Tet2-Tet3* DKO *i*NKT cells. (**a**) ATAC-seq analysis of DARs (red) in wild-type *i*NKT cells versus *Tet2-Tet3* DKO *i*NKT cells: black, DARs that overlap 5hmC (CMS-IP peaks). (**c**) Motif-enrichment analysis (HOMER) of the 3,162 DARs more accessible in *Tet2-Tet3* DKO *i*NKT cells than in wild-type *i*NKT cells (top) and of the 2,711 DARs less accessible in *Tet2-Tet3* DKO *i*NKT cells than in wild-type cells (bottom). (**b**) Distance of DARs to the nearest TSS, among DARs less (blue) or more (red) accessible in *Tet2-Tet3* DKO *i*NKT cells than in wild-type *i*NKT cells or commonly accessible in both wild-type and *Tet2-Tet3* DKO *i*NKT cells (gray). Data are representative of two experiments and three biological replicates per genotype in total for ATAC seq. For CMS-IP, data are representative of one experiment with two biological replicates.

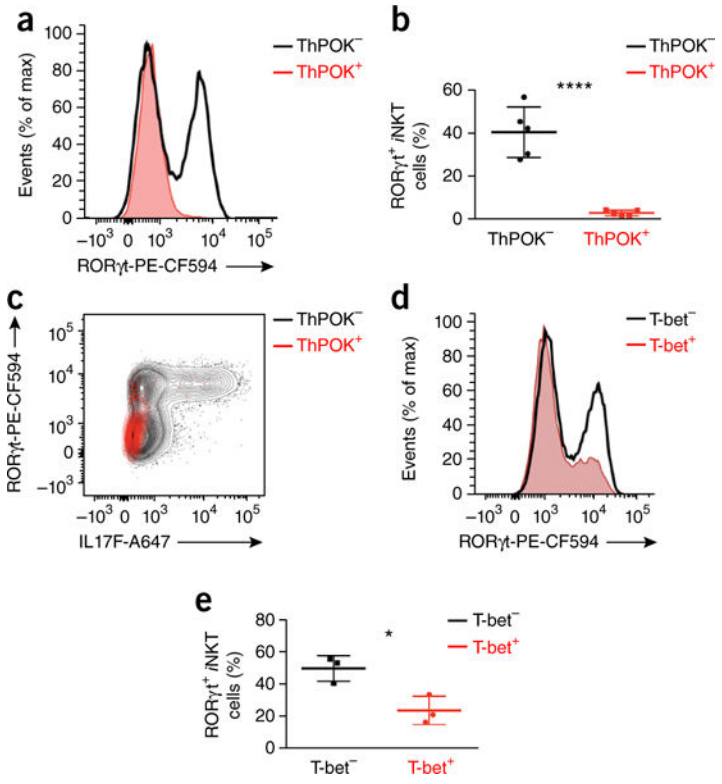

Figure 8.

Ectopic expression of ThPOK or T-bet in *Tet2-Tet3* DKO *i*NKT cells can suppress the aberrant increase in RORγt expression. (**a**) Flow cytometry analysis of RORγt expression in *Tet2-Tet3* DKO *i*NKT cells transduced to express ThPOK (ThPOK$^+$) or not (ThPOK$^-$). (**b**) Frequency of RORγt-expressing *Tet2-Tet3* DKO *i*NKT cells as in **a**. (**c**) Flow cytometry analysis of Rorγt expression and IL-17F production in *Tet2-Tet3* DKO *i*NKT cells as in **a**. (**d**) Flow cytometry analysis of RORγt expression in *Tet2-Tet3* DKO *i*NKT cells transduced to express T-bet (T-bet$^+$) or not (T-bet$^-$). (**e**) Frequency of RORγt-expressing *Tet2-Tet3* DKO *i*NKT cells as in **d**. Each symbol (**b**,**e**) represents an individual mouse; horizontal lines indicate the mean (± s.e.m.). *$P < 0.05$, ****$P < 0.0001$ (unpaired *t* test). Data are representative of four experiments (**a**) or three experiments (**d**) or are from four independent experiments with a total of five mice (**b**), one experiment representative of two experiments with three mice (**c**) or one experiment representative of three experiments (**e**).

Table 1

DMRS (5mC+5hmC) identified by WGBS of wild-type and *Tet2-Tet3* DKO *i*NKT cells

	DMRs	
	DMRs more methylated in *Tet2-Tet3* DKO versus WT *i*NKT cells	**DMRs less methylated in *Tet2-Tet3* DKO versus WT *i*NKT cells**
Total DMRs	10,945	767
DMRs overlapping WT CMS-IP	4,568	10
DMRs overlapping WT CMS-IP close to promoters (±5 kb)	1,468	5
Unique genes from above	1,270	4
Downregulated	138	0
Upregulated	45	3